



Proceedings of the Fifteenth International Conference on
Computational Structures Technology
Edited by: P. Iványi, J. Kruis and B.H.V. Topping
Civil-Comp Conferences, Volume 9, Paper 3.6
Civil-Comp Press, Edinburgh, United Kingdom, 2024
ISSN: 2753-3239, doi: 10.4203/ccc.9.3.6
©Civil-Comp Ltd, Edinburgh, UK, 2024

Optimization Design of a Multifunctional Support Bracket for Nuclear Power Plants

D. Huo and L. Meng

**School of Mechanical Engineering
Northwestern Polytechnical University
Xi'an, China**

Abstract

Over the past several decades, topology optimization has been widely applied in structural design through its integration with fluid mechanics and solid mechanics. This research focuses on the topology optimization design of the support bracket within nuclear fuel assemblies, which is responsible for filtering foreign objects, bearing loads, and facilitating coolant flow. The study initially targets the compliance of the support bracket under multi-point concentrated forces, employing topology optimization techniques to determine the optimal load transfer path. Subsequently, considering the foreign object filtering efficiency of the support bracket, the filtration channel is optimized with the goal of minimizing energy dissipation within the flow path. Finally, an adaptive tessellation strategy is used to integrate the optimized fluid channel with the load-bearing path, resulting in a complete support bracket structure, which is then subjected to structural performance validation. The analysis results indicate that, compared to conventional designs, the topology-optimized bracket has achieved a 17.65% increase in filtering efficiency, a 16.77% reduction in pressure drop, and a 21.88% enhancement in stiffness. These outcomes highlight the robust capabilities and significant potential of topology optimization techniques in the design of multi-functional and integrated structures.

Keywords: topology optimization, additive manufacturing, multi-functionality, load-bearing structure optimization, filter channel optimization, support bracket design

1 Introduction

In nuclear reactors, metallic foreign objects resulting from manufacturing and metal wear can cause damage to the nuclear fuel cladding, leading to the risk of nuclear fuel leakage [1–3]. From 2000 to 2010, a total of 38 nuclear reactors in the United States faced the risk of structural damage to the nuclear fuel cladding due to wear by foreign objects [4]. The lower support bracket, which supports the entire fuel assembly, facilitates the flow of coolant, and filters out foreign objects in the coolant, needs to have sufficient stiffness, high filtering performance, and low pressure drop. Therefore, conducting topological optimization design on the lower support bracket is of significant importance for enhancing the safety of nuclear fuel assemblies.

In the field of structural topology optimization design, Tomlin et al. applied topology optimization techniques in the design of hinge brackets for the Airbus A320 aircraft, achieving a high-performance, lightweight new structure [5]. The cooperative design by Northwestern Polytechnical University and the Third Academy of China Aerospace Science and Industry Corporation, which considered force and thermal loads, resulted in a thermal-elastic topology-optimized bracket with an 18% weight reduction [6]. WU and others used a topology optimization method with stress constraints to design a bracket for an aero-engine, obtaining a model with better quality, strength, and stiffness. SHI and others conducted a thermoelastic topology optimization design for aero brackets considering mechanical forces and temperature loads, achieving a weight reduction of more than 18% while satisfying all constraints [7].

Against the aforementioned background, this paper intends to carry out topological optimization design on the multifunctional lower support bracket in nuclear reactor fuel assemblies.

2 Governing equation

The optimized design of the lower support bracket structure is divided into two parts: one part is the topology optimization design of the load-bearing structure, and the other part is the topology optimization design of the filtering lattice structure that serves to filter foreign objects and facilitate the flow of coolant. The objective functions for these two parts are the minimum compliance response of the lower support bracket structure and the minimum energy dissipation of the filtering flow channel as the optimization goals. Considering the expected weight of the structure, the volume of the load-bearing structure and the volume of the flow channel are used as constraints. The pseudo-density variables of the bracket structure units are updated by the optimization algorithm to achieve the topological evolution of the material layout. The mathematical model for the optimized design of the load-bearing structure of the lower support bracket is shown as Eq.1, and the mathematical model for the optimized design of the filtering flow channel of the lower support bracket is shown as Eq.2.

$$\begin{aligned}
\min_{\rho} C &= \frac{1}{2} \mathbf{F}^T \mathbf{U} \\
\text{s.t. } \mathbf{K} \mathbf{U} &= \mathbf{F} \\
\frac{\sum_{i=1}^a \rho_i V_i}{V} &\leq V_f \\
0 < \rho_i &\leq 1 \quad i = 1, 2, \dots, n
\end{aligned} \tag{1}$$

where ρ_i is the pseudo-density variable, and \mathbf{U} denotes the displacement vector, \mathbf{F} represents the applied load, V_i represents the volume on element i , V represents the total volume of the structure, V_f is the given upper limit of the volume fraction, and δ is an extremely small positive number (10^{-3}) to avoid singularity in stiffness matrix proof.

$$\begin{aligned}
\min \quad \phi &= \int \left[\frac{1}{2} \mu (\nabla \mathbf{u} + \nabla \mathbf{u}^T) : (\nabla \mathbf{u} + \nabla \mathbf{u}^T) + \alpha \mathbf{u} \cdot \mathbf{u} \right] d\Omega \\
\text{subject to } \sum_{i=1}^n V_i \rho_i &\leq f_U V \\
0 < \delta &\leq \rho_i \leq 1
\end{aligned} \tag{2}$$

where ρ_i is the pseudo-density variable, and ϕ represents the energy dissipation of fluid flow, V_i represents the volume on element i , V represents the total volume of the structure, f_u represents the volume fraction of the flow channel and δ is an extremely small positive number (10^{-3}) to avoid singularity in stiffness matrix proof.

3 Typical lower support bracket topology optimization design

The lower support bracket is a key multi-purpose component in the pressurized water reactor (PWR) fuel assembly, as shown in fig.1. Structurally, the lower support bracket bears the weight of the entire fuel assembly. Additionally, it guides the flow of coolant through the filled filtering lattice structure and serves to filter out foreign objects such as metal debris and springs in the coolant, which are produced due to mechanical wear and vibration. Therefore, to enhance the overall performance of the lower support bracket, optimization design needs to be carried out for the load-bearing capacity, foreign object filtering efficiency, and pressure drop performance of the filtering flow channels of the lower support bracket.

In this section, the lower support bracket that has been in operation in the nuclear power plant will be taken as the object of topology optimization design, as shown in fig.2. Topology optimization design will be carried out separately for the filtering unit structure and the load-bearing structure of the lower support bracket; that is, the low-pressure drop flow channel topology optimization design of the filtering unit structure containing the baffle flow channel design domain will be carried out, and the topology

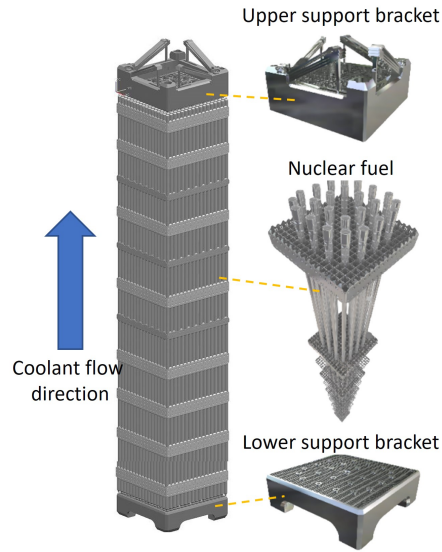


Figure 1: multifunctional bracket on fuel assembly.

optimization design for maximizing stiffness of the load-bearing structure of the lower support bracket will be carried out. In the following text, Section 3.1 introduces the original bracket design model and load conditions. Section 3.2 carries out the pressure drop topology optimization design of the lower support bracket's filtering flow channel with the goal of minimizing pressure drop. Section 3.3 carries out the topology optimization design of the lower support bracket's load-bearing structure with the goal of maximizing stiffness. Finally, Section 3.4 compares the original design with the CAD-reconstructed design.

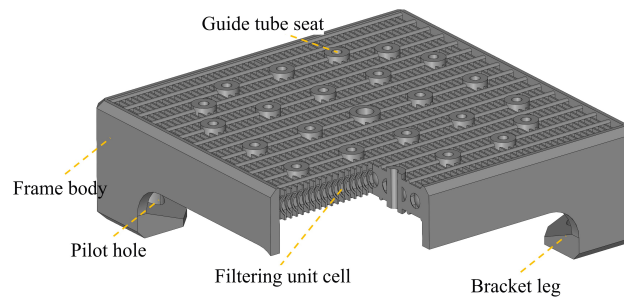


Figure 2: Original lower support bracket structure.

3.1 Original Lower Support Bracket Design and Load Conditions

The original lower support bracket structure is depicted in fig.2, with a weight of 6.0Kg. It can be observed from the figure that to fulfill the structural function of foreign object filtration, the frame body of the structure is filled with filtration lattice. The lower support bracket structure is secured by the positioning pin hole at the bottom,

which is in conjunction with the positioning pin. The weight of the fuel assembly is supported by the 24 guide tube seats on the lower support bracket through the cooperation with the guide tube. Since the weight of the fuel assembly does not change significantly throughout the entire cycle, it can be considered that the load on the lower support bracket is stable. It is assumed that the lower support bracket is made of 304L stainless steel, with material parameters shown in Table 1. The original lower support bracket is discretized using 0.5mm second-order tetrahedral meshes, totaling 3272653, as shown in Fig.3. Abaqus is used to analyze its structural performance, with the analysis results shown in Fig.4. From the figure, it can be seen that the maximum displacement of the structure occurs near the instrument tube seat, measuring 0.32mm, with strain energy E_e at 749.90mJ, and stress concentration appears at the connection point between the filtration unit cell and the guide tube seat. The hydraulic performance is analyzed using Fluent, and the pressure drop contour map is shown in Fig.5. By extracting the inlet and outlet pressures of the original lower support bracket structure, the calculated pressure difference is 17.60KPa.

Table 1: 304L Stainless Steel Material Parameters

Density	Elastic modulus	Poisson's ratio
7.98Kg/cm ³	90GPa	0.3

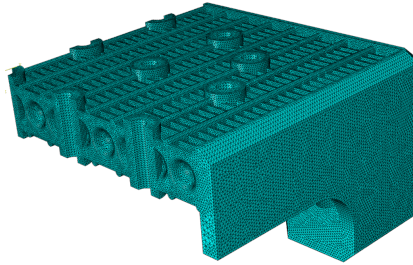


Figure 3: Original Lower Support Bracket Meshing Results.

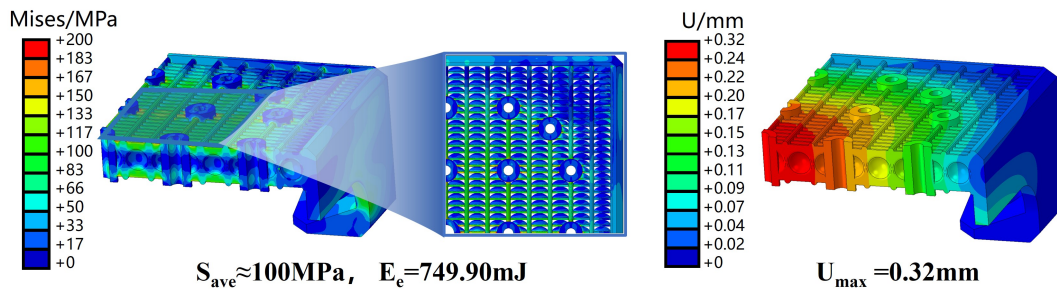


Figure 4: Static Analysis Results of the Original Lower Support Bracket.

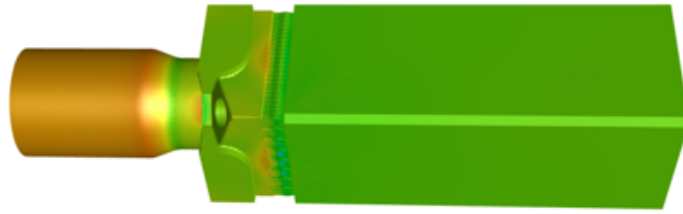


Figure 5: Pressure fields of the original lower support bracket model.

3.2 Design for Minimum Pressure Drop in Lower Support Bracket Filtering Channels

The filtering lattice of the original lower support bracket is depicted in Fig.6. This figure shows that there is a semicircular protrusion at the center of the original filtering lattice structure, which is designed to ensure the structure's capability to filter out foreign objects. To simplify the flow channel of the original filtering lattice, it has been transformed into a two-dimensional model that includes an elliptical protrusion, with the simplification process illustrated in Fig.7. The simplified model is discretized using 12,562 quadrilateral elements, each measuring 0.1mm in size. In this model, the grey area represents the design domain for the fluid, while the black area signifies the non-design domain for the solid material. Referring to the volume of the original filtering lattice, the volume fraction of the flow channel to be preserved is set at 30% . With a filtration radius set to 0.2mm, the objective of the optimization is to minimize the energy dissipation of the fluid flow.

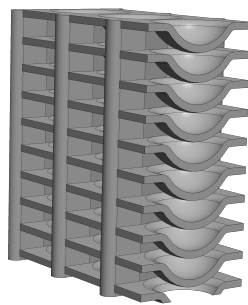


Figure 6: Original filtering lattice structure.

After 26 optimization iterations, the final topological result of the filtering channel was generated, as shown in Fig.8. In the figure, the black part represents the solid material, indicating the walls of the filtering channel; the white area represents the coolant material, signifying the fluid; the red arrows indicate the flow direction of the coolant within the filtering channel, with the size of the arrows representing the velocity of the coolant.

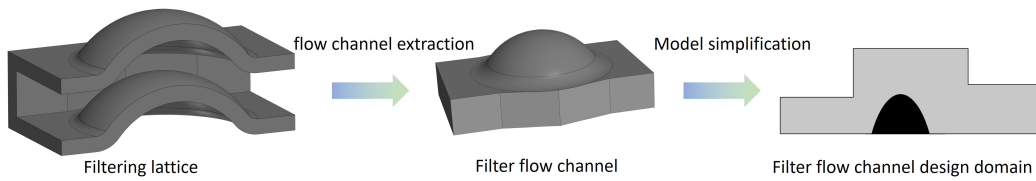


Figure 7: Simplified process of filter flow channel design.

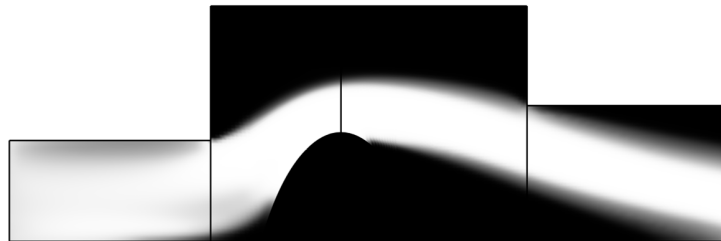


Figure 8: Topology Optimization Results of the Filtering Channel.

3.3 Design for Maximizing the Stiffness of the Lower Support Bracket

The stiffness maximization design of the lower support bracket's load-bearing structure is implemented using the Optistruct design platform with the density method. Initially, pre-processing is conducted on the geometric model of the lower support bracket to expand the design space of the structure. Within Optistruct, the model is discretized into 1,203,340 hexahedral elements, each with a size of 1mm. The red portion in the diagram represents the non-design domain, while the blue portion denotes the design domain, as shown in Fig.9. Referring to the original weight of the structure, the volume fraction of material to be retained is set to 20% of the design domain. The filtration radius is set to 3mm, with a minimum size of 2mm and a maximum size of 6mm. The objective function is to minimize the global compliance of the lower support bracket.

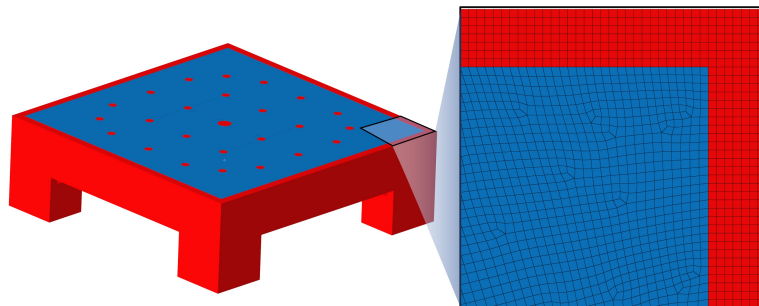


Figure 9: Finite element model of the bracket with extended design domain.

The topology optimization results of the lower support bracket generated by the

Optistruct design platform are shown in Fig.10. After 51 optimization iterations, the final topological structure was achieved. It can be seen from the figure that, within the design domain, intersecting straight ribs were generated to connect the guide tube seats with the frame body.

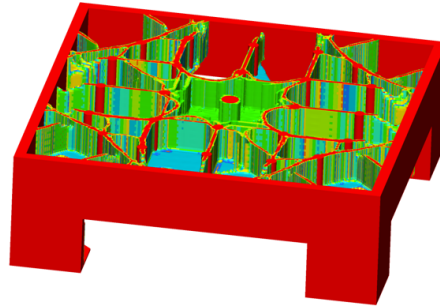


Figure 10: Topology Optimization Results of Load-bearing Path .

4 Model Reconstruction and Verification Analysis

4.1 Model Reconstruction

To compare the performance of the original lower support bracket, the load-bearing structure optimized for stiffness and the filter cell flow channel optimized for pressure drop were reconstructed using CAD geometric modeling tools. Subsequently, the reconstructed filter cell structure was combined with the load-bearing structure to form the optimized lower support bracket. Fig.11 illustrates this reconstruction process, and Fig.12 displays the reconstructed lower support bracket from multiple perspectives.

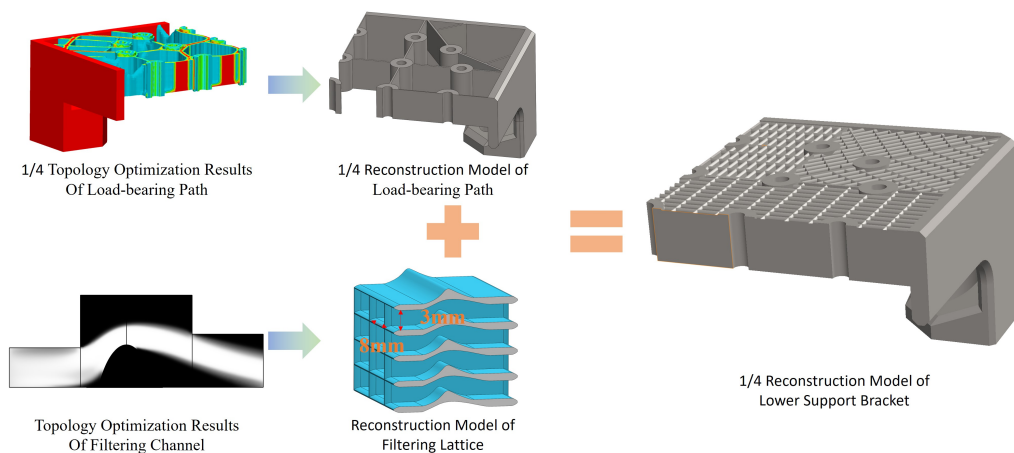


Figure 11: Reconstruction Process of the Lower Support Bracket.

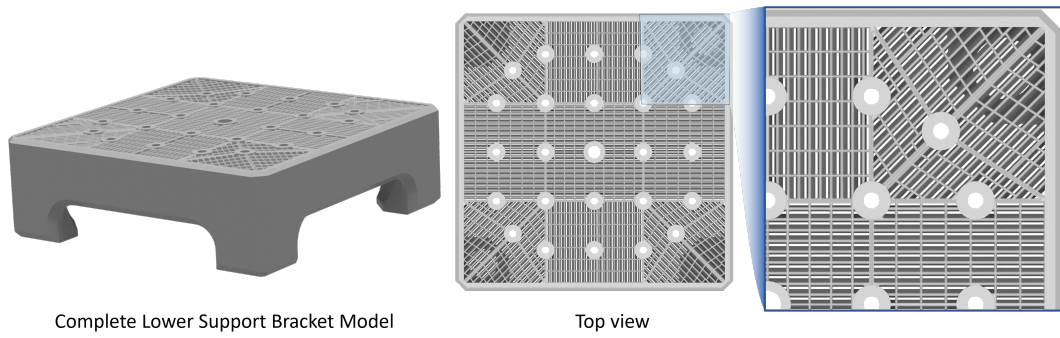


Figure 12: Complete Lower Support Bracket Model.

4.2 Stiffness Verification Analysis

Using ABAQUS, the reconstructed lower support bracket model from Section 4.1 was verified for strength and stiffness. The stress and displacement fields of the lower support bracket under load are depicted in Fig.13. The figure also indicates the strain energy of the structure after loading, which is 585.31J, and the maximum displacement, which is 0.25mm. Compared to the original lower support bracket structure, the strain energy and maximum displacement have been reduced by 21.95% and 21.88%, respectively. Additionally, the average stress is 100MPa.

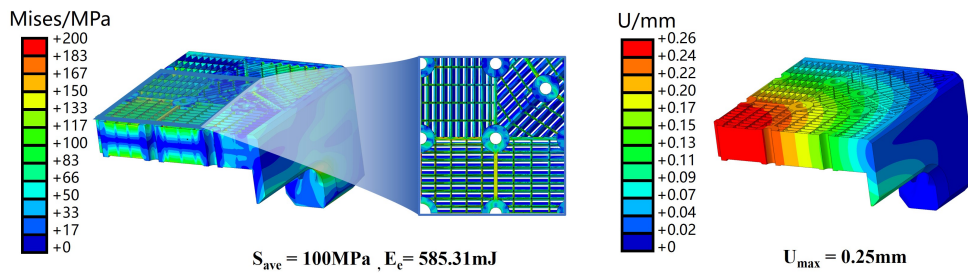


Figure 13: Static Analysis Results of the reconstructed lower support bracket.

To assess the effectiveness of the structural design, this paper selected 20 points with the highest stress for stress linearization treatment. The maximum primary membrane stress calculated was 102.58 MPa, and the maximum primary membrane stress plus bending stress was 160.52 MPa. Both values comply with the standards set by the American Society of Mechanical Engineers (ASME) for reactor vessel design, which specify that the primary membrane stress should be less than 138 MPa and the primary membrane stress plus bending stress should be less than 207 MPa.

4.3 Pressure Drop Verification Analysis

The flow channel structure of the lower support bracket is extracted using CAD software, and the extraction process and results are shown in Fi.14. The pressure drop

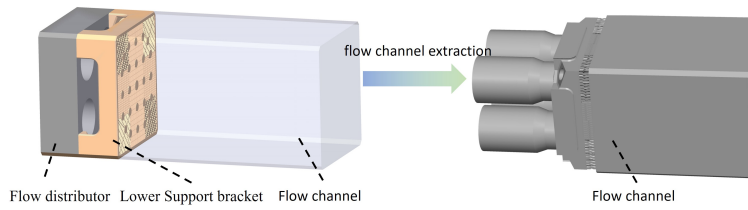


Figure 14: Process of extracting the flow path from the lower support bracket.

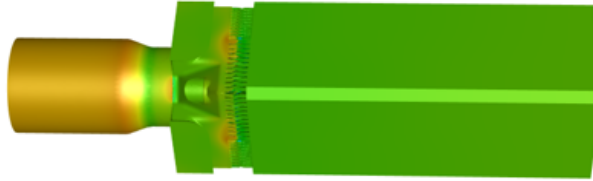


Figure 15: Pressure drop Fields of the reconstructed lower support bracket model.

performance of the lower support bracket is verified using Fluent, and the static pressure nephogram is shown in Fig.15.

Extracting the pressure at the inlet and outlet cross-sections of the lower support bracket flow path, the calculated pressure difference is 14.66 kPa. Compared to the original lower support bracket, the pressure drop has been reduced by 17.65%.

4.4 Filter Performance Verification Analysis

In Section 4.1, the filtration performance of the reconstructed filtration lattice for 34 common foreign objects in the reactor was simulated and analyzed using the coupling technique of Fluent and EDEM. Fig.16 illustrates the trajectory of a cylindrical foreign object with dimensions of $\Phi 1.0mm \times 16mm$ as it changes position within the filtration lattice over time. The results indicate that these sized foreign objects are effectively filtered by the filtration lattice.

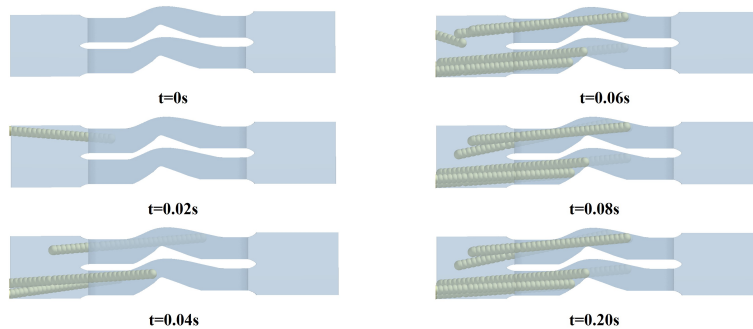


Figure 16: the position of the foreign object changes over time.

The verification results indicate that the optimized filtration lattice can effectively filter 30 out of the 34 foreign objects, achieving a filtration efficiency of 88.24%.

Compared to the original lower support bracket, the filtration efficiency has increased by 17.65% .

5 Conclusion

In this study, a density-based topology optimization method was utilized to optimize the load-bearing structure and filtering channels of the lower support bracket, with the objectives of global minimum compliance and global minimum energy dissipation, respectively. Post-optimization, the results underwent geometric reconstruction and performance verification analysis. The verification results indicate that the maximum displacement of the optimized lower support bracket was reduced by 21.88% , implying a 21.88% increase in stiffness, a 17.05% decrease in pressure drop, and a 17.65% improvement in filtering efficiency.

References

- [1] Min-Su Jung and Kyu-Tae Kim. Debris filtering efficiency and its effect on long term cooling capability. *Nuclear Engineering and Design*, 261:1–9, 2013.
- [2] Nam-Gyu Park, Joon-Kyoo Park, Jae-Ik Kim, and Kyong-Lak Jeon. Pwr fuel debris filtering performance measurement method and its application. *Nuclear Engineering and Design*, 281:96–102, 2015.
- [3] Shuang Deng, Quan-yao Ren, Jing Zhang, Xin Duan, Fa-wen Zhu, Yong Xin, Xin-Yu Yang, Quan Li, and Ying-wei Wu. Numerical simulation analysis of debris filtration in the bottom nozzle. *Annals of Nuclear Energy*, 198:110301, 2024.
- [4] Kyu-Tae Kim. Evolutionary developments of advanced pwr nuclear fuels and cladding materials. *Nuclear Engineering and Design*, 263:59–69, 2013.
- [5] Matthew Tomlin and Jonathan Meyer. Topology optimization of an additive layer manufactured (alm) aerospace part. In *Proceeding of the 7th Altair CAE technology conference*, pages 1–9, 2011.
- [6] Yanfa Wu, Wenke Qiu, Liang Xia, Wenbiao Li, and Kai Feng. Design of an aircraft engine bracket using stress-constrained bi-directional evolutionary structural optimization method. *Structural and Multidisciplinary Optimization*, 64:4147–4159, 2021.
- [7] SHI Guanghui, GUAN Chengqi, QUAN Dongliang, WU Dongtao, TANG Lei, and GAO Tong. An aerospace bracket designed by thermo-elastic topology optimization and manufactured by additive manufacturing. *Chinese Journal of Aeronautics*, 33(4):1252–1259, 2020.